

1 **Assessment of flash flood risk based on improved analytic**
2 **hierarchy process method and integrated maximum**
3 **likelihood clustering algorithm**

4 **Kairong Lin^{1,2,3*}, Haiyan Chen¹, Chong-Yu Xu⁴, Ping Yan², Tian Lan¹, Zhiyong**
5 **Liu^{1,2,3}, and Chunyu Dong^{2,3}**

6 ¹ School of Geography and Planning, Sun Yat-sen University, Guangzhou, China.

7 ² Center for Water Resources and Environment, School of Civil Engineering, Sun
8 Yat-sen University, Guangzhou, China.

9 ³Guangdong Key Laboratory of Oceanic Civil Engineering, Guangzhou, China.

10 ⁴Department of Geosciences, University of Oslo, P.O. Box 1047, Blindern, 0316 Oslo,
11 Norway.

12 *Corresponding author: Kairong Lin (linkr@mail.sysu.edu.cn)

13

14

15

16

17

18 **Abstract**

19 Flash floods are one of the most severe natural disasters throughout the world,
20 and are responsible for sizeable social and economic losses, as well as countless
21 injuries and death. Risk assessment, which identifies areas susceptible to flooding, has
22 been shown to be an effective tool for managing and mitigating flash floods. The
23 study aims to introduce the methods to determine the weights of the risk indices, and
24 identify the different risk clusters. In this regard, we proposed a methodology for
25 comprehensively assessing flash flood risk in a GIS environment, by the improved
26 analytic hierarchy process (IAHP) method, and an integration of iterative
27 self-organizing data (ISODATA) analysis and maximum likelihood (ISO-Maximum)
28 clustering algorithm. The weight for each risk index is determined by the IAHP,
29 which integrates the subjective characteristics with objective attributes of the
30 assessment data. Based on the data mining technology, the integration of
31 ISO-Maximum clustering algorithm derives a more reasonable classification. The
32 Guangdong Province of China was selected for testing the proposed method's
33 applicability, and we used a receiver operating characteristics (ROC) curve approach
34 to validate the modeling of the flash-flood risk distribution. The validation against the
35 historical flash flood data indicates a high reliability of this method for comprehensive
36 flash flood risk assessment. In order to verify the proposed method's superiority, in
37 addition, the technique for order performance by similarity to ideal solution (TOPSIS)

38 and the weights-of-evidence (WE) methods are used for comparison with the IAHP
39 and ISO-Maximum clustering algorithm method. Moreover, we analyzed and
40 compared the regularity of flash floods in the rural and urban areas. This study not
41 only provides a new approach for large-scale flash flood comprehensive risk
42 assessment, but also assists researchers and local decision-makers in designing flash
43 flood mitigation strategies.

44 Keywords: Flash flood Comprehensive risk assessment Improved AHP
45 method ISO-Maximum clustering algorithm Guangdong Province

46 **1 Introduction**

47 The term ‘flash flood’ is commonly defined as rapidly developing floods that
48 begin within 3-6 hr of heavy rainfalls or other triggers (Hapuarachchi et al., 2011). To
49 date, they are considered to be the most widespread, devastating, and abundant
50 naturally occurring disaster. Contemporary climate projections suggest that the
51 occurrence of high-intensity rainfall events will increase in many areas of the globe in
52 the future, and such incidents are the primary cause of extreme flooding (Kvočka et
53 al., 2016). Previous studies suggest that flash floods rank high among the natural
54 disasters that result in large scale damage in China in the 21st century, and they are
55 responsible for approximately 70 deaths and 260 million USD in annual losses
56 (Centre for Research on the Epidemiology of Disasters, 2017). Thus, the ongoing

57 flood risk management is of high importance to reduce casualties and economic losses
58 (Barredo, 2007; Gaume et al., 2009; Marchi et al., 2010).

59 Flood risk assessment is an important flood prevention tool, as it offers
60 significant practical applications in flood risk management and can lead to
61 improvements in public awareness of flood risk (Yang et al., 2018). The flash flood
62 disaster system is complex, and includes disaster-causing factors, disaster-pregnant
63 environments, and disaster-bearing bodies. It has the characteristics of high
64 nonlinearity, spatial-temporal dynamics, and uncertainty, and coupling of various
65 challenges in the system may produce extremely complex phenomena (Wei et al.,
66 2001). Therefore, flash flood risk assessment is a difficult task. Our previous research
67 focused on small-scale flash flood risk assessment based on the TOPMODEL coupled
68 with the 1D-2D hydrodynamic model MIKEFLOOD under the condition of lacking
69 hydro-meteorological data (Li et al., 2019). In this study, we intend to develop a
70 suitable methodology for large-scale flash flood risk assessment despite the data
71 scarcity.

72 In recent years, two typical approaches or theories have been developed and used
73 for deriving regional scientific flood risk maps, i.e. the hydrological-hydraulic
74 modeling (HHM) method and multi-criteria analysis (MCA) method.

75 The classical method for analyzing flood-prone areas with different risk levels is
76 based on the application of hydrological-hydraulic modeling (Cheng et al., 2017; Hu

77 and Song, 2018; Löwe et al., 2017; Mandal and Chakrabarty, 2016; Mani et al., 2014).

78 For example, Mandal et al. (2016) collected data on past rainfall events that triggered

79 flash floods and applied it to build a simulation model. By using HEC-RAS, and

80 HEC-HMS Software, they obtained the peak discharge time and volume, as well as

81 the total inundation area and determined the high flash flood risk in the Sikkim

82 Darjeeling Himalaya Teesta Watershed. Cheng et al. (2017) employed the InfoWorks

83 ICM 2D hydrodynamic model to simulate historical and designed rainfall events, then

84 recorded the simulate water depth and flow velocity for flood risk assessment in the

85 Jinan City. Löwe et al. (2017) linked the 1D-2D hydrodynamic modeling engine

86 MIKE FLOOD (DHI, 2013) with the urban development model DAnCE4-Water

87 (Urich and Rauch, 2014) to consider 9 scenarios for urban development and climate

88 and 32 potential combinations of flood adaptation measures in Melbourne, Australia.

89 Hu and Song (2018) applied the two-dimensional hydrodynamic model to simulate

90 flash flooding in mountain watersheds with a robust finite volume scheme, which can

91 quickly simulate the rainfall-runoff process and be used for real-time prediction of

92 large-scale flash floods with high-resolution grids. Other scholars have applied

93 different hydrological-hydraulic models to carry out numerous and varied studies on

94 flood risk assessment. However, model simulation methods require much more

95 high-quality data, as the relevant calculations are very complex (Wang et al., 2011).

96 Moreover, there are many unmapped large basins where expensive and

97 time-consuming hydrological-hydraulic simulations are not possible due to data
98 scarcity. An additional limitation of the method is that it is not universally applicable
99 to different regions because it depends on the catchment properties (Kourgialas and
100 Karatzas, 2011). In these cases, using an alternative effective tool to delineate the
101 flash flood-prone areas is necessary.

102 Multi Criteria Decision Analysis (MCDA) method is a modeling and
103 methodological tool for dealing with complex problems (He et al., 2018; Shen et al.,
104 2016). Especially, it has been widely used in many studies to assess flood risk
105 (Danumah et al., 2016; Guo et al., 2014; Musungu et al., 2012; Shehata and Mizunaga,
106 2018; Sowmya et al., 2015; Wang et al., 2011). MCA is a broad term used to describe
107 a set of methods that can be applied to support the decision-making processes by
108 considering multiple and often conflicting criteria via a structured framework (Brito
109 and Evers, 2016). The crucial step is to select the methodologies that calculate
110 multiple index weights. Analytic hierarchy process (AHP) method has been applied to
111 flash flood risk assessment with multiple criteria systems (Ghosh and Kar, 2018;
112 Pantelidis et al., 2018; Shehata and Mizunaga, 2018). AHP has a demonstrated ability
113 to assess and map flood risk with good accuracy (Danumah et al., 2016). However,
114 one of the limitations of AHP is its high subjectivity in choosing the weights for each
115 factor since it is significantly affected by the expert's experience and knowledge
116 (Zhao et al., 2017). Thus, some improved AHP methods were further proposed. For

117 example, Xie et al. (2011) proposed an information fusion method based on DS-AHP
118 (Dempster-Shafer and Analytic Hierarchy Process) to deal with uncertainty
119 information. Zou et al. (2013) introduced fuzzy mathematics in which AHP was
120 combined with trapezoidal fuzzy numbers to calculate assessment indices' weights.
121 Guo et al. (2014) determined the assessment indices weights by combining the
122 minimum relative entropy principle and the AHP. Zhao et al. (2015) introduced game
123 theory to correct the one-sidedness of the single weighting method by integrating AHP
124 weight and entropy weight. Fang et al. (2017) built Grey-AHP model based on the
125 grey theory to overcome uncertainty resulted from determination of some indices'
126 weight. Dahri and Abida (2017) built a function of weights using Monte Carlo
127 simulation and global sensitivity analysis to improve the AHP. However, these
128 methods need a lot of detailed data, and the computation processes for all the above
129 methods are complicated and tedious.

130 Given the above concerns, the purpose of this study is to propose an integrated
131 method based upon the IAHP method and ISO-Maximum likelihood clustering
132 algorithm for large-scale flash flood risk assessment under conditions of data scarcity.
133 Due to intelligible theories and simple implementation steps, the proposed method
134 offers general applicability. Performing large-scale flash flood risk assessment in
135 China and other developing countries is of great significance, as it can guide
136 stakeholders and government officials to focus on areas prone to flash flood disasters

137 and improve regional management and planning efficiency. IAHP is a comprehensive
138 method for determining weights of the assessment indices, which combines the AHP
139 weight method and the entropy method to reflect empirical judgments of experts and
140 objective variability of assessment data. Furthermore, in order to determine the risk
141 level of different regions, we adopted the ISO-Maximum likelihood clustering
142 algorithm to conduct clustering analysis. The clustering analysis algorithm is a data
143 mining technology and thus overcomes the difficulty in determining the risk
144 classification threshold that is required in traditional flood risk analysis (Xu et al.,
145 2018). Finally, we verified the assessment results qualitatively and quantitatively
146 using the historical data from flash flood disasters. In previous studies, most
147 researchers tended to qualitatively verify the flash flood assessment results (Shehata
148 and Mizunaga, 2018; Zou et al., 2013), so quantitative validation of assessment results
149 is rarely found. Thus, the receiver operating characteristic technique (ROC) is
150 introduced to quantitatively evaluate the established model's accuracy, which is
151 widely used to assess model accuracy in landslide vulnerability (Bednarik et al., 2010;
152 Bui et al., 2011), groundwater qanat potential (Naghibi et al., 2015), and flash flood
153 susceptibility (Khosravi et al., 2018). ROC is flexible enough for a range of
154 capabilities, and provides a trial for the quantitative validation of the flash flood risk
155 assessment model. Through the above steps, we obtained a reasonable flash flood risk
156 distribution map of the study area. The cartographic products are very useful for

157 helping decision-makers and map users from various fields (such as strategic planning,
158 emergency management, or the public) adapt appropriate actions and measures for
159 flood risk mitigation (Godfrey et al., 2015; Meyer et al., 2012).

160 Additionally, TOPSIS and WE methods were selected for comparison with the
161 IAHP and ISO-Maximum likelihood clustering algorithm. TOPSIS is extensively
162 applied to water resource and environmental problems (Zagonari and Rossi, 2013), as
163 well as flood risk analysis in previous literature (Chengjie et al., 2017; Lee et al., 2014;
164 Najafabadi et al., 2016; Radmehr and Araghinejad, 2015). The WE method is also
165 adapted to flood or landslide risk research and has achieved reasonable results in
166 interesting areas (Xu et al., 2012; Tehrany et al., 2014; Weed, 2010). Subsequently, we
167 obtained the results through TOPSIS and WE methods, then compared and discussed
168 the similarities and differences obtained by the three methods.

169 The remainder of this paper is structured as follows. Section 2 introduces the
170 study area and data; while Section 3 shows how we adapted the IAHP method and the
171 ISO-Maximum clustering algorithm for comprehensive flash flood risk assessment.
172 Section 4 displays detailed results of the trial region. In Section 5 we present a series
173 of discussions on the implementation and improvement of the proposed method.
174 Finally, the conclusions are summarized in Section 6.

175 **2 Study area and data**

176 2.1 Study area

177 Guangdong Province is located on the southernmost tip of China. It includes the
178 Pearl River Delta, which is one of China's most important economic development
179 zones and is an important part of the Guangdong-Hong Kong-Macao Greater Bay
180 Area for the national development strategy. Guangdong Province is situated at
181 $20^{\circ}13'-25^{\circ}31'N$, $109^{\circ}39'-117^{\circ}19'E$ and covers an area of $179,700 \text{ km}^2$ (Figure 1). It is
182 vulnerable to flash floods because of its unusual geographic location and complex
183 topography. Guangdong Province is one of the wettest areas in China, with an average
184 annual precipitation of 1789 mm. Drainage systems are numerous and complex, and
185 primarily consist of Pearl River, Han River, and many other smaller rivers. In addition,
186 the topography in Guangdong Province is characterized by mountains, hills, platforms,
187 valleys, basins, and plains interlacing with each other. All these above natural
188 conditions tend to facilitate the occurrence of flash floods.

189 Statistical analysis shows that flash floods in Guangdong Province have occurred
190 in 1182 small watersheds since 1980, in 15 of 69 counties (cities and districts). They
191 have covered an area of $116,800 \text{ km}^2$ and affected a population of 27,177,400 people.
192 About 3.85 million people are regularly threatened by flash floods, of which 3.08
193 million are living in rural areas and 0.77 million are in towns and cities. Flash floods
194 also directly threaten the safety of industrial and mining enterprises and important
195 infrastructure with fixed assets of 98.99 billion RMB. Therefore, it is critical to

196 establish a suitable flash flood risk assessment model for regional safety and
197 development.

198 **2.2 Data**

199 Three types of data were collected for the proposed method in this study: 1) basic
200 administrative division of the study area; 2) the flash flood risk assessment indices,
201 including the Digital Elevation Model (DEM) data, terrain slope (SL), rainfall,
202 drainage, topographic, population, economic, and urbanization data; and 3) records of
203 historical flash flood events, which are used to verify the assessment results accuracy.
204 The above data are described in detail in section 1 of the supplementary material.

205 **3 Methodology**

206 The overall framework of the proposed method involves two main components:

207 (1) The IAHP method and the ISO-Maximum likelihood clustering algorithm
208 were used to develop the flash flood risk levels map (Figure 2).

209 (2) In order to verify the proposed method that was applied to flash flood risk
210 assessment, the distribution map of historical flash flood disasters was employed to
211 qualitatively verify evaluation results and ROC curves were introduced to
212 quantitatively assess the model accuracy.

213 3.1 Conceptual model

214 Various studies have used different definitions of risk. This study establishes a
215 conceptual model based on District Disaster System theory (Shi, 1996; Crichton and
216 Mounsey, 1997). The definition of risk is expressed by Eq. 1 (Maskrey, 1989) :

$$217 \quad \text{Risk} = \text{Hazard} + \text{Vulnerability} \quad (1)$$

218 where *Hazard* is the premise, which mainly describes the natural environment
219 and hydro-climatic conditions in the assessment area. *Vulnerability* represents
220 socio-economic conditions in the region and describes the potential losses. *Risk*
221 indicates the probability and potential loss based on different intensity floods.
222 Therefore, we adopt a general structure in which risk is a function of both the hazard
223 and vulnerability of the indices at risk. Thus, the conceptual model of regional flash
224 flood risk assessment can be expressed as:

$$225 \quad R = f(H, V) \quad (2)$$

226 where

$$227 \quad H = f(h) = \sum_{i=1}^n \omega_i h_i \quad (3)$$

$$228 \quad V = f(v) = \sum_{j=1}^m \omega_j v_j \quad (4)$$

$$229 \quad R = f(H, V) = \sum_{i=1}^n \omega_i h_i + \sum_{j=1}^m \omega_j v_j \quad (5)$$

230 where h_i and v_j represent hazard and vulnerability indices values, respectively,
231 after standardization treatments. ω_j and ω_i are the hazard and vulnerability index
232 weights, respectively.

233 3.2 IAHP method

234 a. Selection of risk indices

235 Flood risk occurrence is a combination of natural and anthropogenic factors, and
236 the selection of risk index variables varies among study areas according to the specific
237 characteristics of each location (Tehrany et al., 2013). After carefully considering the
238 flash flood characteristics associated with hazard and vulnerability in the study area
239 and reviewing the recommendations throughout the literature, we selected eight
240 indices based on available data. The four hazard indices consist of: drainage density
241 (DD), comprehensive rainstorm (CR), slope (SL), and topography (TO); while the
242 four vulnerability indices are: urbanization ratio (UR), population density (PD),
243 primary industry proportion (PIP), and per unit area GDP (PUAGDP). The basic data
244 and detailed process of the eight criteria have showed in the Supplementary Material
245 (Figure S1), all the abbreviations used in.

246 b. Calculation of weight

247 AHP, developed by Saaty (1980), is one of the best known and most widely used
248 multi-criteria analysis (MCA) approaches. Furthermore, the AHP method has been
249 shown to comprehensively determine weights by considering the data's subjective
250 attributes (Xu et al., 2018). In contrast, entropy is a management approach employed
251 in the system to prevent disorder, instability, disturbance, and uncertainties inherent in

252 that system (Pourghasemi et al., 2014). Entropy offers a method for estimating main
 253 factors among effective factors of an objective. In other words, it determines variables
 254 that are more influential in event occurrence (Haghizadeh et al., 2017). Thus, IAHP
 255 combines the subjectivity of AHP and the objectivity of the entropy weight method to
 256 comprehensively determine the weights of indices. The specific steps for performing
 257 this calculation are as follows:

258 (1) Entropy weight method to determine weights of risk indices.

259 Step1: Assuming that there are m objects and n indices, the judgment matrix R is
 260 constructed.

$$261 \quad R = (r_{ij})_{m \times n} \quad (6)$$

262 Step2: The matrix R is transformed into a normalized matrix R' to avoid the
 263 effect of the different evaluation data units.

$$264 \quad R' = (r'_{ij})_{m \times n} \quad (7)$$

265 The specific normalization formulas are as follows:

266 (a) Normalized formula for positive indices:

$$267 \quad r'_{ij} = \frac{r_{ij} - \min(r_{ij})}{\max(r_{ij}) - \min(r_{ij})} \quad (8)$$

268 (b) Normalized formula for negative indices:

$$269 \quad r'_{ij} = \frac{\max(r_{ij}) - r_{ij}}{\max(r_{ij}) - \min(r_{ij})} \quad (9)$$

270 Step3: The entropy e_j of the j th index is defined as follows:

$$271 \quad e_j = \frac{-\sum_{i=1}^m f_{ij} \ln f_{ij}}{\ln m} \quad (10)$$

272 where $f_{ij} \ln f_{ij}$ is set as zero if f_{ij} is equal to zero and

$$273 \quad f_{ij} = r_{ij} / \sum_{i=1}^m r_{ij} \quad i=1,2,3,\dots,m; j=1,2,3,\dots,n \quad (11)$$

274 Step4: The entropy weight ω_1 is calculated as follows:

$$275 \quad \omega_1 = 1 - e_j \quad (12)$$

276 (2) AHP method to determine the weights of risk indices

277 The AHP method uses hierarchical structures to represent the problem, and then
278 develops the priorities for alternatives based on the user's judgment. The main steps in
279 implementing the AHP method are as follows (Saaty, 1980):

280 Step1: Break a complex unstructured problem down into its component factors.

281 Step2: Develop the AHP hierarchy, the AHP model used in the process flash
282 flood risk map is shown in Table 1.

283 Step3: Design a paired comparison matrix determined by imposing judgments.

284 In the study, we invited relevant experts to determine the relative degree of
285 importance between risk indices, which is the basis for the construction of the
286 judgment matrix (Table 2).

287 Step4: Assign values to subjective judgments and calculate the relative weights

288 of each criterion. The binary combination for index comparison in Table 3 is based on
289 a scale proposed by Saaty (1980).

290 Step5: Synthesize judgments to determine the priority variables.

291 Step6: Check the consistency of assessments and judgments. If the consistency
292 ratio is < 0.1 , then the mentioned matrix can be considered as an acceptable
293 consistency.

294 (3) IAHP method to determine the final weights

295 The determination of index weight should maximize the balance between
296 subjective intention and objective impartiality to evaluate the results, so the
297 calculation of the final weight ω by the IAHP is as follows (Wang, 2018):

$$298 \qquad \qquad \qquad \omega = 0.5\omega_1 + 0.5\omega_2 \qquad \qquad \qquad (13)$$

299 Where ω_2 denotes the subjective weight determined by the AHP method.

300 c. Making risk assessment index layers

301 The geographic information system (GIS)-based method employs a spatial
302 analysis function for flood risk assessment, and forms visual flood risk maps to provide
303 useful information for decision-makers (DMs) and insurance companies (Wang et al.,
304 2011). This study mainly uses the ArcGIS Spatial Analysis module function to make
305 the risk assessment index layers. The specific processing steps are detailed in section 2
306 of the supplementary material.

307 **3.3 ISO-Maximum Likelihood algorithm clustering analysis**

308 Clustering is a popular data analysis and data mining technique, which aims at
309 partitioning a collection of data objects into several groups or clusters, such that
310 intra-cluster dissimilarity is small and inter-cluster dissimilarity is large. In this study,
311 the ISODATA clustering algorithm and the maximum likelihood algorithm were
312 combined for risk clustering analysis. The ISODATA is a widely used partitioning,
313 unsupervised and iterative clustering algorithm. The fundamental difference between
314 the ISODATA clustering algorithm and the traditional clustering algorithm is that the
315 former is a soft classification while the latter is a hard one. Soft classification can
316 recognize the most essential attributes, and most classification objects are unlikely to
317 show during the initial cognition or initial classification (Yang and Luo, 2006; Zeng,
318 2009). A more detailed explanation concerning the ISODATA clustering algorithm
319 calculation principle is available in Memarsadeghi et al. (2007).

320 Furthermore, the feature file generated by the ISODATA clustering algorithm is
321 used as the input file for the Maximum likelihood clustering classification, which can
322 better control the classification parameters. All the above steps are completed by GIS
323 techniques, enabling the study to obtain more scientific clustering results for flash flood
324 risk.

325 3.4 Verification

326 In this study, we conducted both qualitative and quantitative validation of the
327 assessment results. To begin the qualitative verification, we normalized the historical
328 data of flash flood events, then summed the normalized values to generate the historical
329 flash flood loss distribution map in the GIS environment. The qualitative verification
330 analysis was realized by comparing the historical flash flood loss map with the risk
331 distribution map. In contrast, the ROC was introduced to quantitatively evaluate the
332 proposed method's accuracy, which has rarely done in previous studies. The ROC
333 curve is a statistical technique that can be used to provide performance predictions and
334 compare different models (sensitivity vs. specificity) (Bui et al., 2011) , by depicting a
335 graphical representation of equilibrium between the negative and positive rate of error
336 for each possible fitness value (Pourghasemi et al., 2014). The curve is a
337 two-dimensional graph, in which the true-positive rate is plotted on the Y-axis and the
338 false-positive rate is plotted on X-axis. The area under the ROC curve (AUC) is a
339 summary of the plot's information, which can be used to estimate the validity: accuracy
340 or overall quality of the model (Hosmer and Lemeshow, 2000). If the AUC value is
341 close to 1, the model accuracy is considered to be high (Bui et al., 2011). In this study,
342 we selected two representative flood events, including extreme precipitation events
343 during June 2005 and June 2010. The data from these events were entered into the

344 established risk assessment model and used to forecast flash flood likelihood as well as
345 plot the ROC curves to realize quantitative accuracy analysis.

346 **4 Results**

347 **4.1 Weights**

348 Based on the detailed description in Section 3.2, the index weights were
349 calculated using the IAHP method, which mainly integrates the entropy weight and
350 the AHP method. To begin, the entropy weights of risk indices in the study area were
351 calculated, as shown in Table 4. The results in Table 5 indicate that the judgment
352 matrices pass the consistency test. Table 4 shows that the weight results determined by
353 the entropy weight and the AHP method are significantly different, so it is more
354 reasonable to adopt the IAHP method, which comprehensively considers the
355 subjective judgment and objective data variability. The final index weights are listed
356 in Table 4. According to the final calculation results, the established evaluation model
357 can be determined as follows:

$$358 \quad R = f(H, V) = \sum_{i=1}^n \omega_i h_i + \sum_{j=1}^m \omega_j v_j = 0.134SL + 0.046DD + 0.136CRV + \\ 359 \quad 0.077TO + 0.064UR + 0.179NPD + 0.076PIP + 0.289PUGDP \quad (14)$$

360 where R is risk, H is hazard, and V is vulnerability, h_i and v_j represent values
361 of the hazard and vulnerability indices, respectively, after standardization treatments,

362 while ω_j and ω_i are the weights for the hazard and vulnerability indices,
363 respectively.

364 **4.2 Risk distribution**

365 The risk index layer's distribution map was developed using the GIS techniques
366 (more detailed data of the study area are given in section 1 of the supplementary
367 material). Furthermore, following the above calculation steps, we determined the final
368 weight of each index and multiplied it in classes of that index or values related to each
369 index. Weighted maps were added up and final maps of flash flood hazard,
370 vulnerability, and risk were obtained (Figures 3.a.b.c). Finally, the risk clustering map
371 was generated based on the ISO-Maximum likelihood clustering algorithm (Figure
372 3.d).

373 A flash flood risk distribution map that only considers the hazard indices should
374 be different from one considering both the hazard and vulnerability indices. In general,
375 both maps have similar space patterns: the risk in the northern low mountainous areas
376 is higher than the southern plain, and the difference in some parts of the study area is
377 greatly influenced by the socio-economic indices. Some high-level flash flood areas
378 showed a low-risk level when the socio-economic indices were considered, e.g.,
379 Qujiang, Huidong, and Lechang. In these cases, fewer people, properties and primary
380 industries are located in the areas with a high flood hazard level. As such, the
381 casualties and property losses are expected to be lower, even though the risk of

382 flooding is high. On the contrary, some areas with a low flash flood hazard level have
383 significantly high-risk for damage, e.g., Shenzhen, Guangzhou, Yangxi, and Huilai. If
384 a flash flood occurs in these areas, there will be a large number of casualties and
385 property losses due to the dense populations and high property concentrations.
386 Therefore, a comprehensive flash flood risk map acts more representative of the study
387 area due to the involvement of hazard and vulnerability.

388 According to the results of flash flood risk clustering, three categories of flash
389 flood risk were compared: low, medium, high. As shown in Figure 3.d, low, medium,
390 and high-risk zones accounted for 12.51%, 38.59%, and 48.91%, respectively. The
391 high-risk areas are mainly located in the north, east and southwest parts of Guangdong
392 Province, and the areas with the highest flash flood risk occurred in Guangzhou and
393 Baoan.

394 The mean index value of the three risk levels was calculated in order to analyze
395 the underlying causes of the risk distribution (Figure 4). As shown in Figure 4, the
396 high-risk zones generally exhibit higher slopes and are distributed over low
397 mountainous and hilly regions. Disaster-causing vulnerability indices, including
398 higher PIP and lower UR more easily induce the flash floods. Thus, the combination
399 of physical and socio-economic variables could result in a high flash flood risk.

400 Furthermore, Figure 5 shows 8 index values for each of the 20 selected areas in
401 the high risk zones: Xuwen, Qingxin, Zijin, Xinfeng, Lianzhou, Wuhua, Xingning,

402 Renhua, Dongyuan, Shixing, Longmen, Yangchun, Liannan, Wengyuan, Huaiji,
403 Yingde, Lianshan, Yangdong, Yangshan, Longgang, Yangxi. As demonstrated in
404 Figure 5, all the selected areas generally exhibit higher SL and PIP and lower UR.
405 Moreover, most of the areas are located in low mountain regions. It is also evident
406 from Figure 5 that most high-risk areas have higher CRV and DD values than the
407 other areas. In general, high-risk areas tend to have higher slopes, more rainfall, and
408 developed primary industry, a lower urbanization rate, and be located in mountainous
409 regions. These counties (districts) should be a priority for carrying out intensive
410 studies and considering flash flood mitigation measures.

411 The regularity of flash flooding in the study area was further analyzed by
412 selecting and comparing 20 typical urban and rural areas. The 8 index values of each
413 selected area are shown in Figures 6 and 7, and were used to analyze the main
414 disaster-causing factors. The results demonstrated that the main flash flood
415 disaster-causing factors in rural areas (Figure 7) show more regularities than urban
416 areas (Figure 6), which may indicate that the assessment system based on the IAHP
417 method is more suitable for mountainous areas. For these areas, the flash flood
418 disaster-causing factors include low-lying terrain (such as middle and low
419 mountainous areas), lower UR and higher SL, which is consistent with the flash flood
420 formation theories. The flash flood formation theories emphasize that the terrain in
421 mountainous rural areas is undulating, and the windward side of the mountains

422 provides sufficient water for flash floods. Furthermore, the steep mountains provide
423 dynamic conditions for downward sliding, which is conducive to the rapid
424 accumulation of flash flood waters into valleys. Although the disaster-causing factors
425 of flat urban areas do not depict universal laws, we find high-risk urban areas due to
426 higher rainfall concentrations. Normally, flash flooding directly in urban areas is
427 caused by intense rainfall events, which exceed the capacity of the drainage systems
428 (Blanc et al., 2012; Maksimović et al., 2009). Moreover, inadequate solid-waste
429 management and drain maintenance can lead to clogged drains, which in turn leads to
430 localized flooding even with light rainfall (Satterthwaite et al., 2007).

431 **4.3 Verification**

432 The flash flood historical loss distribution map was derived using the method
433 detailed in the supplementary material (Figure S2), and then overlapped with the flash
434 flood risk distribution map in Figure 8. Results showed that the middle, high-risk areas
435 cover the counties (districts) with severe historical flash flood losses, which
436 preliminarily demonstrates the reliability and rationality of the assessment results. The
437 data also showed that the risk to developed areas along the coast is overestimated,
438 mainly because of excessively abundant rainfall and the concentrated population and
439 economy.

440 Next, the ROC curves were plotted based on the true-positive and flash-positive
441 degree of identified flash floods as the classification threshold varies. According to the

442 two ROC curves, the AUCs were 0.693 and 0.729 for the selected flash flood events
443 (Figure 9). This indicates that the established flash flood assessment model has
444 relatively good accuracy.

445 In summary, we obtained relatively reasonable and reliable risk assessment results
446 for Guangdong Province using the IAHP and ISO-Maximum likelihood clustering
447 algorithm. Furthermore, the results were verified as described above. Thus, the flash
448 flood risk map exhibits practical application in regional unity planning and flash flood
449 prevention in the Guangdong Province.

450 **5 Discussions**

451 **5.1 Comparison of methods**

452 The TOPSIS method and EW method were compared to the IAHP method to
453 validate the proposed approach in flash flood risk assessment. Figures 10 and 11
454 present the flash flood risk maps developed by the TOPSIS and EW methods.

455 Using the TOPSIS method, we produced a risk distribution similar to the
456 assessment results of the IAHP and ISO-Maximum clustering algorithm. In addition,
457 the flash flood risk spatial distribution is approximately identical to the PIP
458 distribution map, more detailed data of study area are displayed in section 1 of
459 supplementary material (Figure S1.g). Furthermore, the proportion of high-risk zones
460 is extremely low (approximately 11.17%), and the maximum and minimum risk

461 values are higher and lower, respectively, than the results of our proposed method. In
462 addition, by comparing the distribution maps of historical flash floods disaster losses,
463 it becomes clear that the risk of many flash flood disaster-prone areas in northeast and
464 west of Guangdong Province, such as Gaozhou, Huazhou, Wuhua, Zijin, Dongyuan,
465 etc., is obviously underestimated. This comparison indicates that the assessment
466 results from the TOPSIS method are potentially problematic and inferior to the
467 method proposed in this paper.

468 For the flash flood risk distribution, there are noticeable differences between the
469 EW method and the IAHP method. The results shown in Figure 11 are simply
470 unreasonable, as they indicate that the high-risk areas are located in the southwest and
471 east of Guangzhou, while the risk in the northern mountainous areas is lower.
472 Furthermore, comparison with the distribution of the historical flash flood losses
473 indicates that the risk in northern Guangdong Province is obviously underestimated.
474 These results show that the IAHP method is more reasonable than the EW method.

475 **5.2 Advantages and limitations**

476 The IAHP and ISO-Maximum likelihood clustering algorithm were proposed to
477 assess large-scale flash flood risk and were applied to the Guangdong Province as a
478 case study. The results show that the proposed framework can achieve more reliable
479 results in large-scale flash flood risk assessment. The methodology has the following
480 advantages: (1) The model's construction theory is intelligible. The theoretical basis

481 of the model is flash flood risk formation mechanisms, which builds a conceptual
482 model from two aspects of vulnerability and hazard. (2) The IAHP method is adapted
483 to effectively determine the weights of different risk indices. It takes the objective
484 characteristics of data and the empirical judgment of experts into account. (3) Data
485 mining technology ISO-Maximum likelihood clustering algorithm is used for
486 clustering analysis, which overcomes the deficiency in traditional flash flood risk
487 classification and obtains more reasonable classification results. (4) A series of
488 appropriate operations in the GIS environment improved situations where data deficits
489 originally limited evaluation of flash flood risk, with high efficiency and flexibility.

490 However, the proposed approach also has some limitations. In large-scale studies,
491 a regional economic development gap will lead to a great change in social
492 vulnerability indices data, and the weights of vulnerability indices are slightly
493 overestimated by the proposed method. The regional economic development of the
494 study area is extremely unbalanced, as the Pearl River Delta region is more developed,
495 while other regions are less developed. Therefore, the variation range of vulnerability
496 indices is much larger than that of the hazard indices, which results in the weights of
497 vulnerability indices being overestimated by the IAHP method. This is also part of the
498 reason why the risk in economically developed areas, such as Shenzhen and
499 Guangzhou, is overestimated. In the future, this problem can be improved by
500 acquiring more detailed data and increasing relative risk indices. Moreover, more

501 detailed work would focus on waterlogging disasters in these urban cities in the future
502 (Yang et al., 2019; Zhu et al., 2019).

503 When compared to other alternatives, the proposed method has greater
504 reproducibility and applicability, and can obtain relatively good evaluation results
505 based on basic theories and simple operation processes. There are reasons to believe
506 that this method will offer preferable assessment results with the support of high
507 accuracy and abundant data.

508 **5.3 Improvement**

509 Based on our study, the following measures should be considered to further
510 improve the IAHP and ISO-Maximum likelihood clustering algorithm in flash flood
511 risk assessment:

512 First, physical and social vulnerability factors should be taken into account when
513 analyzing regional vulnerability (Karagiorgos et al., 2016). In this study, only the
514 physical vulnerability was considered with the socio-economic and demographic
515 indicators. More social vulnerability factors are expected in order to improve
516 assessment accuracy, including residency length, the degree of solidarity, the trust of
517 people living in the area, and participation in local associations, etc. (Hurlbert et al.,
518 2000; Kuhlicke et al., 2011).

519 Second, the variables that trigger flash floods are complex. Accordingly, it is less

520 reasonable to adopt a unified evaluation index system, and risk indices should be
521 determined based on the different regional characteristics.

522 Third, in order to compute the overall risk, weights calculated by the AHP and
523 entropy method are given equal weight, but some adjustments may be needed in the
524 future studies. The huge gap in regional socio-economic development will lead to
525 overestimation of the vulnerability factor weights. Hazard indices are the source for
526 flash floods. If there was no adverse environment to form flash floods, then no loss
527 would be induced, and the region would not suffer hazards.

528 Finally, numerous studies focus on flash flood risk in spatial dimension rather
529 than temporal. Thus, determining how to effectively integrate real-time information to
530 establish a dynamic flash flood risk assessment model in the future is currently a hot
531 issue (Adams et al., 2019, Shirisha et al., 2019, Zhang et al., 2019a, Zhang et al.,
532 2019b). There is no doubt that flash flood assessment will be strengthened by
533 collaboration with other disciplines, such as radar technology and remote sensing.

534 **5.4 Prevention of flash floods**

535 This study indicates that most areas in Guangdong Province are encountering
536 high or medium flash flood risks; thus some kinds of appropriate methods are needed
537 to mitigate flash flood risk. Mitigation measures vary, ranging from physical measures,
538 such as flood defense or safe building design, to legislation, and training and

539 improving public awareness. Public officials are suggested to provide some flood
540 control engineering supports in flood-prone areas, such as embankment construction
541 and channel improvement, etc. Furthermore, flash flood risk maps have been shown to
542 greatly support planners and engineers to select suitable locations for implementation
543 of flash flood control measures. For Guangdong Province, the government should also
544 focus on renovating aging and damaged flood control facilities. These measures can
545 provide substantial protection for flash floods in areas prior to such events.

546 Furthermore, flash flood warning systems (FFEW) present a more efficient
547 approach to flood prevention and mitigation than engineering measures (Li et al.,
548 2018), which can provide real-time forecasting based on developed technologies. The
549 government should increase the density of weather, rainfall, and river monitoring
550 networks and develop radar and satellite technology for acquiring high-quality
551 real-time data. Moreover, the government should also expand the options enabling the
552 masses to receive and share real-time flash flood information-e.g., creating relative
553 applications (APPs).

554 Protecting people from flash flood disasters is a race against time (Li et al., 2018),
555 as in many areas, the question is not if it will happen, but when. In addition to
556 delivering real-time and useful information, it is also important to improve human
557 response to flash flood disasters. These approaches should be considered for
558 enhancing the public's ability to cope with flash floods, such as promoting the

559 knowledge of flash flood escape routes and conducting regular flood control exercises
560 and evacuation drills.

561 By using a combination of the above measures, we believe that the flash flood
562 risk can be effectively mitigated, thus reducing the devastation caused by flash floods
563 to human society.

564 **6 Conclusions**

565 Flash flood risk assessment is unquestionably helpful for avoiding and/or reducing
566 death and destruction from flooding. In addition, knowledge and scientific
567 understanding of flash flood risk distribution are clearly beneficial to policymakers, as
568 well as the public. The study provides a new approach for large-scale flash flood
569 comprehensive risk assessment with data scarcity, which integrates IAHP with
570 ISO-Maximum clustering algorithm. In the proposed method, the IAHP approach was
571 used to determining the weights of risk indices, which additionally considers entropy
572 weights to modify the subjectivity of traditional AHP. It is the important step to realize
573 a comprehensive assessment. The ISO-Maximum likelihood clustering algorithm was
574 used to resolve the artificial determination of the flash flood risk clusters' threshold,
575 which could obtain more reasonable classification results. Besides, the ROC curve
576 was introduced to evaluate the accuracy of flash flood risk assessment model
577 quantitatively, which was rarely shown in previous studies. Conclusions are drawn as
578 follows:

579 (1) The good agreement between the assessment results and historical spatial
580 patterns of the flash flood events indicates that the IAHP and ISO-Maximum
581 clustering algorithm method exhibits good suitability for practical applications.

582 (2) The results of the study area indicate that flash flood risk of Guangdong
583 Province is classified into three categories: low, medium, and high. Most of the
584 areas are located in middle- or high-risk level, and high-risk zones account for
585 48.91% of total area. In general, the assessment result matches well with the
586 historical data of flood events. Meanwhile, the credibility and reliability of the
587 results derived from the proposed method are obvious as compared with the
588 TOPSIS and WE methods.

589 (3) We further analyzed the regularity of flash flooding through the assessment
590 results in the study area. The high-risk blocks mainly cover in the north, east and
591 southwest of study area. The main indices cause the high-risk including higher
592 SL, CRV, lower UR and complex terrain. For rural areas, the flash flood
593 disaster-causing factors include low-lying terrain, lower UR and higher SL.
594 Higher rainfall concentrations are the disaster-causing factor to flash flood of
595 urban areas where are more prone to waterlogging disasters.

596 **Acknowledgments**

597 This study is financially supported by the Excellent Young Scientist Foundation

598 of NSFC (51822908), the National Natural Science Foundation of China (No.
599 51779279), the National Key R&D Program of China (2017YFC0405900), the
600 Baiqianwan project's young talents plan of special support program in Guangdong
601 Province (42150001), and the Research Council of Norway (FRINATEK Project
602 274310). Digital Elevation Model (DEM) of the study area is derived from the
603 Advanced Spaceborne Thermal Emission and Reflection Radiometer (ASTER) global
604 digital elevation model (GDEM) with a cell size of 90×90 m which are obtained
605 from <https://asterweb.jpl.nasa.gov/>.

606 **References**

- 607 Adams, T.E., Dymond, R.L., 2019. Possible hydrologic forecasting improvements resulting from
608 advancements in precipitation estimation and forecasting for a real-time flood forecast system
609 in the Ohio River Valley, USA. *Journal of Hydrology*, 579.
610 DOI:10.1016/j.jhydrol.2019.124138.
- 611 Barredo, J.I., 2007. Major flood disasters in Europe: 1950–2005. *Natural Hazards*, 42(1): 125-148.
- 612 Bednarik, M., Magulová, B., Matys, M., Marschalko, M., 2010. Landslide susceptibility
613 assessment of the Kral'ovany–Liptovský Mikuláš railway case study. *Physics & Chemistry of
614 the Earth Parts A/b/c*, 35(3): 162-171.
- 615 Blanc, J. et al., 2012. Enhanced efficiency of pluvial flood risk estimation in urban areas using
616 spatial-temporal rainfall simulations. *Journal of Flood Risk Management*, 5(2): 143-152.
617 DOI:10.1111/j.1753-318X.2012.01135.x

618 Brito, M.M.D., Evers, M., 2016. Multi-criteria decision-making for flood risk management: A
619 survey of the current state of the art. *Natural Hazards Earth System Sciences*, 16(4):
620 1019-1033.

621 Bui, D.T., Revhaug, I., Dick, O., 2011. Landslide susceptibility analysis in the Hoa Binh province
622 of Vietnam using statistical index and logistic regression. *Natural Hazards*, 59(3): 1413-1444.

623 Cheng, T., Xu, Z.X., Hong, S.Y., Song, S.L., 2017. Flood Risk Zoning by Using 2D
624 Hydrodynamic Modeling: A Case Study in Jinan City. *Math. Probl. Eng*, 1-8.
625 DOI:10.1155/2017/5659197.

626 Chengjie, Y. et al., 2017. Flood hazard analysis method based on complex network approach & its
627 application. *Journal of Natural Disasters*, 26(3): 48-55.

628 Crichton, D., Mounsey, C., 1997. How the insurance industry will use its flood research.
629 *Proceedings of the Third MAFF Conference of Coastal and River Engineers*: 131–134.

630 Dahri, N., Abida, H., 2017. Monte Carlo simulation-aided analytical hierarchy process (AHP) for
631 flood susceptibility mapping in Gabes Basin (southeastern Tunisia). *Environmental Earth*
632 *Sciences*, 76(302): 1-14.

633 Danumah, J.H. et al., 2016. Flood risk assessment and mapping in Abidjan district using
634 multi-criteria analysis (AHP) model and geoinformation techniques, (cote d’ivoire).
635 *Geoenvironmental Disasters*, 3(10): 1-13. DOI:10.1186/s40677-016-0044-y.

636 Fang H., W.C., Chao G., 2017. Urban Rainstorm Waterlogging Risk Assessment Based on
637 GreyAHP. *Kongzhi yu Juece/Control and Decision*: 210-224.

638 Gaume, E. et al., 2009. A compilation of data on European flash floods. *Journal of Hydrology*,
639 367(1): 70-78.

640 Ghosh, A., Kar, S.K., 2018. Application of analytical hierarchy process (AHP) for flood risk
641 assessment: a case study in Malda district of West Bengal, India. *Natural Hazards*, 94(1):
642 349-368.

643 Godfrey, A., Ciurean, R.L., van Westen, C.J., Kingma, N.C., Glade, T., 2015. Assessing
644 vulnerability of buildings to hydro-meteorological hazards using an expert based approach -
645 An application in Nehoiu Valley, Romania. *International Journal of Disaster Risk Reduction*,
646 13: 229-241. DOI:10.1016/j.ijdrr.2015.06.001

647 Guo, E., Zhang, J., Ren, X., Zhang, Q., Sun, Z., 2014. Integrated risk assessment of flood disaster
648 based on improved set pair analysis and the variable fuzzy set theory in central Liaoning
649 Province, China. *Natural Hazards*, 74(2): 947-965.

650 Haghizadeh, A., Siahkamari, S., Haghiabi, A.H., Rahmati, O., 2017. Forecasting flood-prone areas
651 using Shannon's entropy model. *Journal of Earth System Science*, 126(39): 1-16.

652 Hapuarachchi, H.A.P., Wang, Q.J., Pagano, T.C., 2011. A review of advances in flash flood
653 forecasting. *Hydrological Processes*, 25(18): 2771-2784.

654 He, L., Shen, J., Zhang, Y., 2018. Ecological vulnerability assessment for ecological conservation
655 and environmental management. *Journal of Environmental Management*, 206: 1115-1125.

656 Hosmer D.W., Lemeshow S., 2000. *Applied logistic regression*, 2nd edn. A Wiley-Interscience
657 Publication. New York.

658 Hu, X., Song, L., 2018. Hydrodynamic modeling of flash flood in mountain watersheds based on
659 high-performance GPU computing. *Natural Hazards*, 91(2): 567-586.

660 Hurlbert, J.S., Haines, V.A., Beggs, J.J., 2000. Core Networks and Tie Activation: What Kinds of
661 Routine Networks Allocate Resources in Nonroutine Situations? *American Sociological*
662 *Review*, 65(4): 598-618.

663 Karagiorgos, K., Thaler, T., Heiser, M., Hübl, J., Fuchs, S., 2016. Integrated flash flood
664 vulnerability assessment: Insights from East Attica, Greece. *Journal of Hydrology*, 541:
665 553-562.

666 Khosravi, K. et al., 2018. A comparative assessment of decision trees algorithms for flash flood
667 susceptibility modeling at Haraz watershed, northern Iran. *Science of the Total Environment*,
668 627: 744-755.

669 Kourgialas, N., Karatzas, G., 2011. Flood management and a GIS modelling method to assess
670 flood-hazard areasâ a case study. *International Association of Scientific Hydrology Bulletin*,
671 56(2): 212-225.

672 Kuhlicke, C., Scolobig, A., Tapsell, S., Steinführer, A., Marchi, B.D., 2011. Contextualizing social
673 vulnerability: findings from case studies across Europe. *Natural Hazards*, 58(2): 789-810.

674 Kvočka, D., Falconer, R.A., Bray, M., 2016. Flood hazard assessment in areas prone to flash
675 flooding, Egu General Assembly Conference.

676 Lai, C.G. et al., 2015. A fuzzy comprehensive evaluation model for flood risk based on the
677 combination weight of game theory. *J Natural Hazards*, 77(2): 1243-1259.

678 Lee, G., Jun, K.S., Chung, E.S., 2014. Robust spatial flood vulnerability assessment for Han River
679 using fuzzy TOPSIS with α -cut level set. *Expert Systems with Applications*, 41(2): 644-654.

680 Li, H., Lei, X., Shang, Y., Tao, Q., 2018. Flash flood early warning research in China. *International*
681 *Journal of Water Resources Development*, 34(3): 369-385.

682 Li, W.J. et al., 2019. Risk assessment and sensitivity analysis of flash floods in ungauged basins
683 using coupled hydrologic and hydrodynamic models. *Journal of Hydrology*, 572: 108-120.
684 DOI:10.1016/j.jhydrol.2019.03.002.

685 Löwe, R. et al., 2017. Assessment of Urban Pluvial Flood Risk and Efficiency of Adaptation
686 Options Through Simulations – A New Generation of Urban Planning Tools. *Journal of*
687 *Hydrology*, 550: 355-367. <http://dx.doi.org/10.1016/j.jhydrol.2017.05.009>.

688 Maksimović, P.Č. et al., 2009. Overland flow and pathway analysis for modelling of urban pluvial
689 flooding. *Journal of Hydraulic Research*, 47(4): 512-523.

690 Mandal, S.P., Chakrabarty, A., 2016. Flash flood risk assessment for upper Teesta river basin:
691 using the hydrological modeling system (HEC-HMS) software. *Modeling Earth Systems*
692 *Environmental Earth Sciences*, 2(2): 1-10.

693 Mani, P., Chatterjee, C., Kumar, R., 2014. Flood hazard assessment with multiparameter approach
694 derived from coupled 1D and 2D hydrodynamic flow model. *Natural Hazards*, 70(2):
695 1553-1574.

696 Marchi, L., Borga, M., Preciso, E., Gaume, E., 2010. Characterisation of selected extreme flash
697 floods in Europe and implications for flood risk management. *Journal of Hydrology*, 394(1-2):

698 118-133.

699 Maskrey, A., 1989. Disaster mitigation: a community based approach. Oxford England Oxfam.

700 Memarsadeghi, N., Mount, D.M., Netanyahu, N.S., Moigne, J.L., 2007. A Fast Implementation of
701 the isodata Clustering Algorithm. International Journal of Computational Geometry &
702 Applications, 01(17): 71-103.

703 Meyer, V. et al., 2012. Recommendations for the user-specific enhancement of flood maps. Nat.
704 Hazards Earth Syst. Sci., 12(5): 1701-1716. DOI:10.5194/nhess-12-1701-2012

705 Musungu, K., Motala, S., Smit, J., 2012. Using Multi-criteria Evaluation and GIS for Flood Risk
706 Analysis in Informal Settlements of Cape Town: The Case of Graveyard Pond. South African
707 Journal of Geomatics, 1: 78-91.

708 Naghibi, S.A., Pourghasemi, H.R., Pourtaghi, Z.S., Rezaei, A., 2015. Groundwater qanat potential
709 mapping using frequency ratio and Shannon's entropy models in the Moghan watershed, Iran.
710 Earth Science Informatics, 8(1): 171-186.

711 Najafabadi, R.M. et al., 2016. Identification of natural hazards and classification of urban areas by
712 TOPSIS model (case study: Bandar Abbas city, Iran). Geomatics Natural Hazards Risk
713 Analysis, 7(1): 85-100.

714 Pantelidis, P., Pazarskis, M., Karakitsiou, A., Dolka, V., Taxation, 2018. Modeling an Analytic
715 Hierarchy Process (AHP) assessment system for municipalities in Greece with public
716 accounting of austerity. Journal of Accounting, 10(5): 69-79.

717 Pourghasemi H.R., Moradi H.R., Fatemi A.S.M., 2014. Prioritizing factors affecting landslide and

-
- 718 zonation of its susceptibility using Shannon's entropy index, *Soil Water Sci.* 70: 181–191.
- 719 Radmehr, A., Araghinejad, S., 2015. Flood Vulnerability Analysis by Fuzzy Spatial Multi Criteria
720 Decision Making. *Water Resources Management*, 29(12): 4427-4445.
- 721 Saaty, T. L. 1980. *The Analytic Hierarchy Process: Planning, Priority setting, Resource allocation*,
722 Mc Graw-Hill, New York, 19.
- 723 Satterthwaite, D., Huq, S., Reid, H., Pelling, M., Lankao, P.R., 2007. *Adapting to Climate Change*
724 *in Urban Areas. Human Settlements Discussion Paper Series.*
- 725 Shehata, M., Mizunaga, H., 2018. Flash Flood Risk Assessment for Kyushu Island, Japan.
726 *Environmental Earth Sciences*, 77(76): 1-20.
- 727 Shen, J., Lu, H., Zhang, Y., Song, X., He, L., 2016. Vulnerability assessment of urban ecosystems
728 driven by water resources, human health and atmospheric environment. *Journal of Hydrology*:
729 536(2016):457-470.
- 730 Shi, P., 1996. THEORY AND PRACTICE OF DISASTER STUDY. *Journal of Natural Disasters*.
- 731 Shirisha, P., Reddy, K.V., Pratap, D., 2019. Real-Time Flow Forecasting in a Watershed Using
732 Rainfall Forecasting Model and Updating Model. *Water Resources Management*.
733 DOI:10.1007/s11269-019-02398-2.
- 734 Sowmya, K., John, C.M., Shrivasthava, N.K., 2015. Urban flood vulnerability zoning of Cochin
735 City, southwest coast of India, using remote sensing and GIS. *Natural Hazards*, 75(2):
736 1271-1286.
- 737 Tehrany, M.S., Pradhan, B., Jebur, M.N., 2013. Spatial prediction of flood susceptible areas using

738 rule based decision tree (DT) and a novel ensemble bivariate and multivariate statistical
739 models in GIS. *Journal of Hydrology*, 504(8): 69-79.

740 Tehrany, M.S., PRADHAN, Biswajeet, Jebur, M.N., 2014. Flood susceptibility mapping using a
741 novel ensemble weights-of-evidence and support vector machine models in GIS. *Journal of*
742 *Hydrology*, 512(6): 332-343.

743 Urich, C., Rauch, W., 2014. Exploring critical pathways for urban water management to identify
744 robust strategies under deep uncertainties. *Water Research*, 66: 374-389.

745 Wang, Y., Li, Z., Tang, Z., Zeng, G., 2011. A GIS-Based Spatial Multi-Criteria Approach for Flood
746 Risk Assessment in the Dongting Lake Region, Hunan, Central China. *Water Resources*
747 *Management*, 25(13): 3465-3484.

748 Wang, Y., 2018. Study on Risk Zoning of Mountain Flood Disaster in Gansu Loess Plateau Based
749 on GIS and Comprehensive Weighting Method Rural Water Conservancy and Hydropower in
750 China 8: 118-122. (in Chinese)

751 Weed, D.L., 2010. Weight of evidence: a review of concept and methods. *Risk Analysis*, 25(6):
752 1545-1557.

753 Wei, Y., Fan, Y., Jin, J., 2001. Systematic theory of flood hazard risk analysis. *Journal of*
754 *Management Sciences in China*, 4(2): 7-11.

755 Xie, Y., Yi, S., Cao, Y., Lu, Y., 2011. Uncertainty information fusion for flood risk assessment
756 based on ds-ahp method. *International Conference on Geoinformatics*: 1-6.

757 Xu. C., et al., 2012. Landslide hazard mapping using GIS and weight of evidence model in

758 Qingshui River watershed of 2008 Wenchuan earthquake struck region. Earth Science
759 (English), 23(1): 97-120.

760 Xu, H., Chao, M., Lian, J., Xu, K., Chaima, E., 2018. Urban flooding risk assessment based on an
761 integrated k-means cluster algorithm and improved entropy weight method in the region of
762 Haikou,China. Journal of Hydrology, 563: 975-986.

763 Yang, X.M., Luo, Y., 2006. Implementation and Analysis of ISODATA algorithm. Mining
764 Technology, 02: 66-68. (in Chinese)

765 Yang, W., Xu, K., Lian, J., Bin, L., Ma, C., 2018. Multiple flood vulnerability assessment
766 approach based on fuzzy comprehensive evaluation method and coordinated development
767 degree model. Journal of Environmental Management, 213: 440-450.

768 Yang, S.Y. et al., 2019. Research on the emergency management pattern and adjustment system for
769 urban waterlogging. IOP Conference Series: Earth and Environmental Science, 344: 012094 (7
770 pp.)-012094 (7 pp.). DOI:10.1088/1755-1315/344/1/012094

771 Zagonari, F., Rossi, C., 2013. A heterogeneous multi-criteria multi-expert decision-support system
772 for scoring combinations of flood mitigation and recovery options : with environment data
773 news. Environmental Modelling Software, 49(11): 152-165.

774 Zeng, J.Y., 2009. Principle and Implementation of ISODATA Algorithm. Science Mosaic, 07:
775 126-127. (in Chinese)

776 Zhang, G. et al., 2019a. Real-time monitoring and estimation of the discharge of flash floods in a
777 steep mountain catchment. Hydrological Processes, 33(25): 3195-3212.

778 DOI:10.1002/hyp.13551

779 Zhang, Y. et al., 2019b. Effectiveness of aerial and ISERV-ISS RGB photos for real-time urban
780 floodwater mapping: case of Calgary 2013 flood. *Journal of Applied Remote Sensing*: 13(4).
781 DOI:10.1117/1.Jrs.13.044521

782 Zhao, H., Yao, L., Mei, G., Liu, T., Ning, Y., 2017. A Fuzzy Comprehensive Evaluation Method
783 Based on AHP and Entropy for a Landslide Susceptibility Map. *Entropy*, 19(396): 1-16.
784 DOI:10.3390/e19080396.

785 Zhu, X. et al., 2019. A dynamic impact assessment method for rainstorm waterlogging using
786 land-use data. *Journal of Integrative Environmental Sciences*, 16(1): 163-190.
787 DOI:10.1080/1943815x.2019.1707232

788 Zou, Q., Zhou, J., Zhou, C., Song, L., Guo, J., 2013. Comprehensive flood risk assessment based
789 on set pair analysis-variable fuzzy sets model and fuzzy AHP. *Stochastic Environmental
790 Research Risk Assessment*, 27(2): 525-546.

791

792 **List of Tables**

793 **Table 1**

794 AHP hierarchy model of the study area

Goal		Flash flood risk		
Criteria		Hazard		Vulnerability
		CRV		PD
		TO		UR
Index		SL		PUAGDP
		DD		PIP

795

796 **Table 2**

797 Judgment matrices in AHP

Hazard-Vulnerability			Hazard-Index				Vulnerability-Index					
H	V		CRV	TO	SL	DD	PD	UR	PUAGDP	PIP		
H	1	3/2	CRV	1	5/2	15/14	3	PD	1	3/2	1	3/2
			TO	2/5	1	3/7	6/5	UR	2/3	1	2/3	1
			SL	14/15	7/3	1	14/5	PUAGDP	1	3/2	1	3/2
V	2/3	1	DD	1/3	5/6	5/14	1	PIP	2/3	2	2/3	1

798

799 **Table 3**

800 Index comparison based on binary combination Saaty (1980)

Scale	Judgment of preference	Description
1	Equal Importance	Two factors contribute equally to the objective
3	Moderate Importance	Experience and judgment slightly favor one over the other
5	Essential Importance	Experience and judgment strongly important favor one over the other
7	Very/strong Importance	Experience and judgment strongly important favor one over the other
9	Extreme Importance	The evidence favoring one over the other is of the highest possible validity
2,4,6,8	Intermediate preference between adjacent scales	When compromised is needed

801

802 **Table 4**

803 Determination of the index weights of assessment indices

Methods	Index							
	SL	DD	CRV	TO	UR	PD	PIP	PUAGDP

AHP	0.210	0.075	0.225	0.090	0.080	0.120	0.080	0.120
Entropy weight	0.057	0.017	0.046	0.064	0.049	0.238	0.072	0.457
Improved AHP	0.134	0.046	0.136	0.077	0.064	0.179	0.076	0.289

804

805 **Table 5**

806 The consistency test matrices by the relative experts for flash flood risk
807 assessment.

Judge matrix	λ_{max}	m	RI	CI	CR	Consistency
H-V	2	2	\	0	0	Yes
Hazard-Index	4	4	0.89	0	0	Yes
Hazard-Index	4	4	0.89	0	0	Yes

808 λ_{max} , m, RI, CR and CI represent the judgment matrix' largest eigenvalue, order,
809 random consistency indicator, random consistency index and consistency ratio,
810 respectively.

811

812

813

814

815

816 **List of Figures**

817 Figure 1 Location and administrative divisions of study area, Guangdong
818 province consists of 21 prefecture-level cities and 37 counties (districts).

819 Figure 2 The overall framework of flash flood assessment.

820 Figure 3 Spatial distribution of flash flood vulnerability, hazard, risk and risk
821 clusters in study area.

822 Figure 4 Mean normalized index values of the assessment indices of different
823 risk levels.

824 Figure 5 Normalized index values of the assessment indices of selected areas in
825 the high risk level.

826 Figure 6 Normalized index values of the assessment indices of the selected
827 urban areas in the high risk level.

828 Figure 7 Normalized index values of the assessment indices of the selected
829 rural areas in the high risk level.

830 Figure 8 Verification result. Comparison between historical disaster losses and
831 risk distribution of flash flood.

832 Figure 9 ROC curves of flash flood potential forecasting map. The left ROC
833 curve map is the forecasting result of the extreme precipitation events during the June
834 2005, and the right is the extreme precipitation events during the June 2010.

835 Figure 10 Spatial distribution of flash flood risk is developed by the TOPSIS
836 method in study area.

837 Figure 11 Spatial distribution of flash flood risk is developed by the EW
838 method in study area.

839

840

841

842

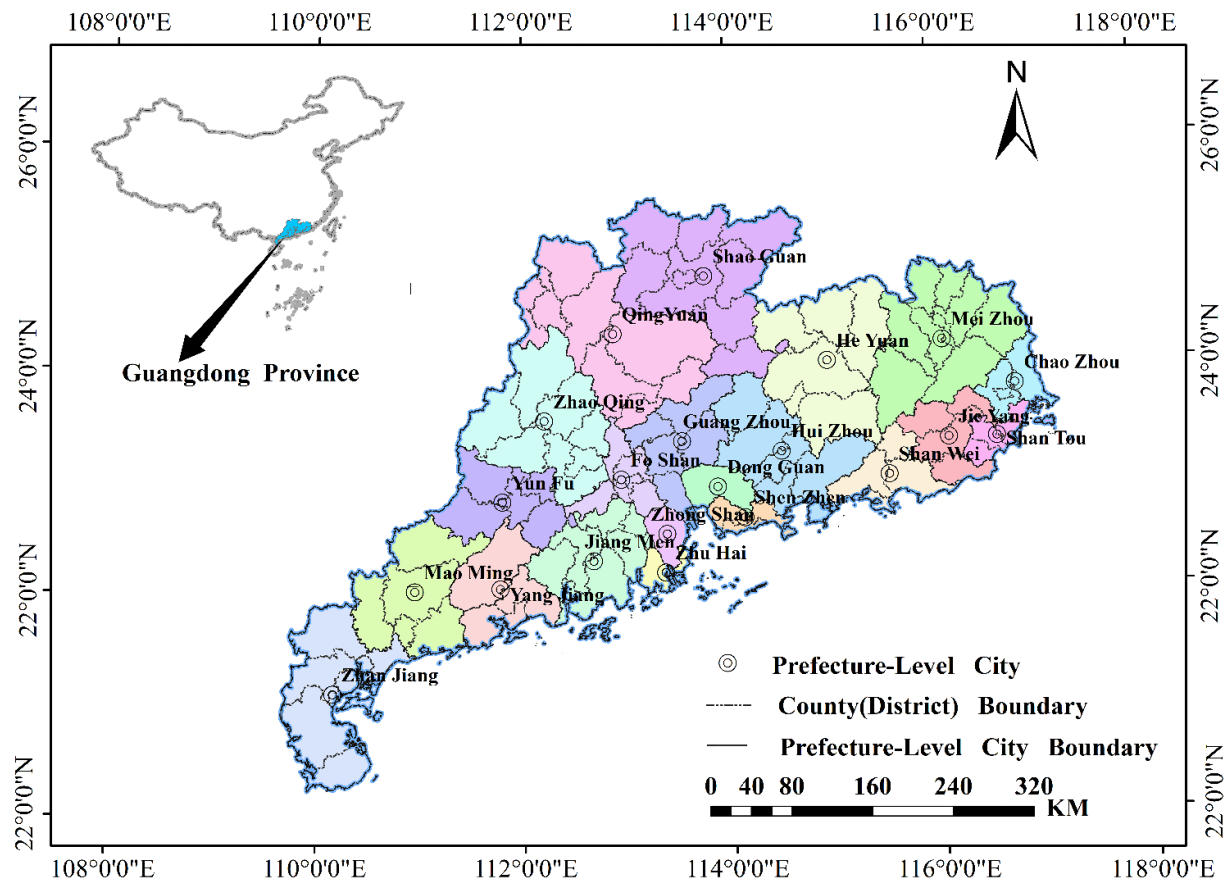
843

844

845

846

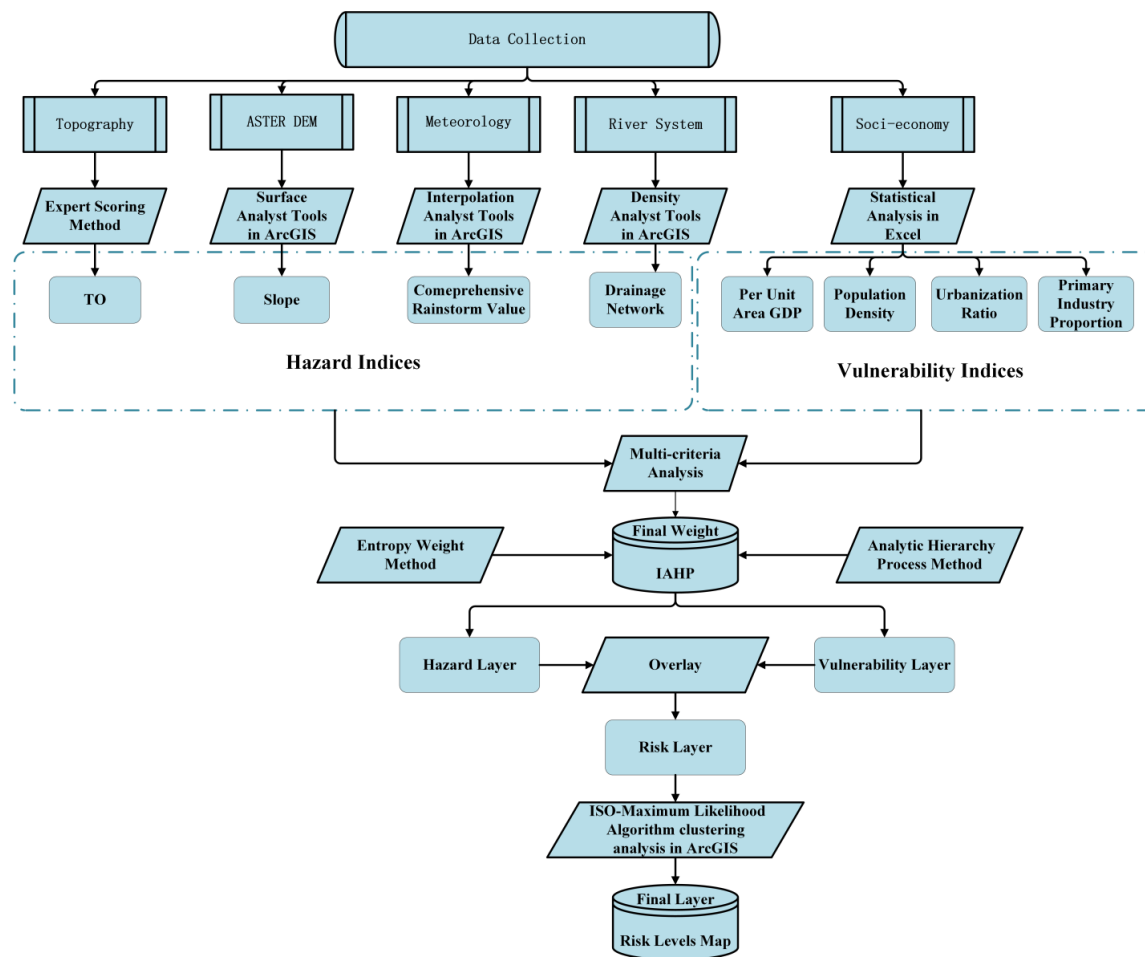
847



848

849

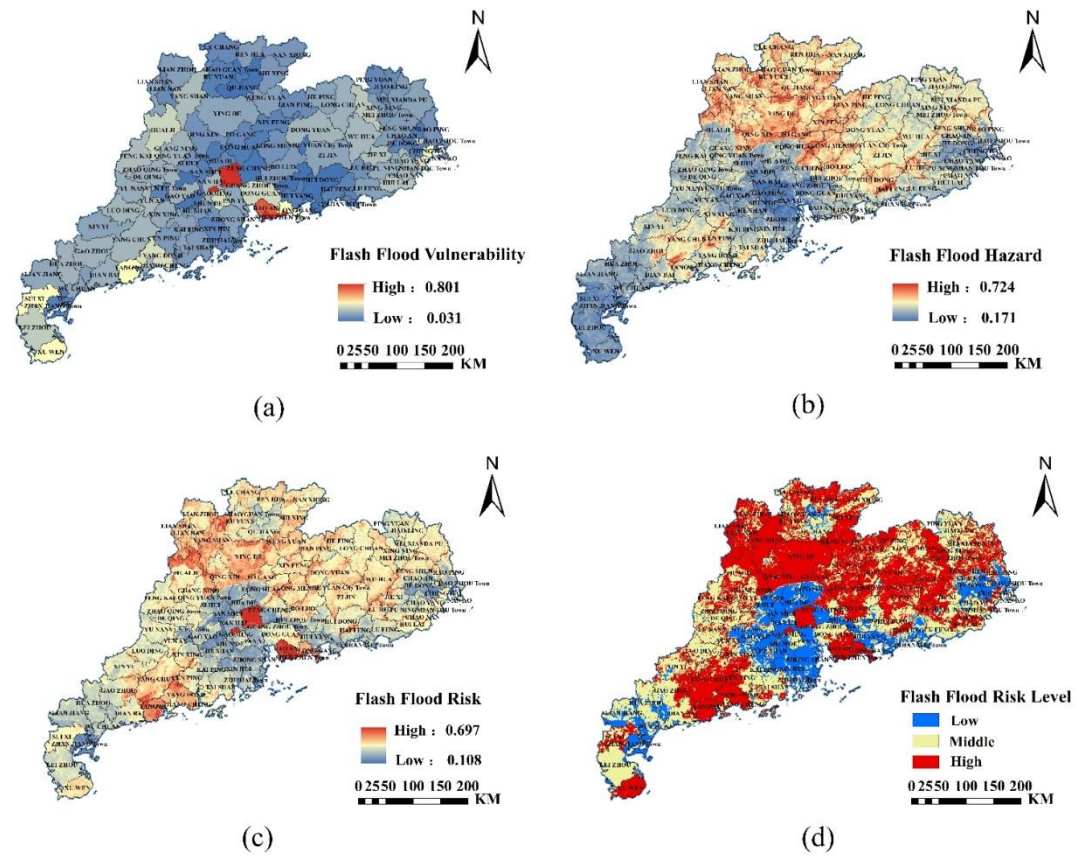
Figure 1



850

851

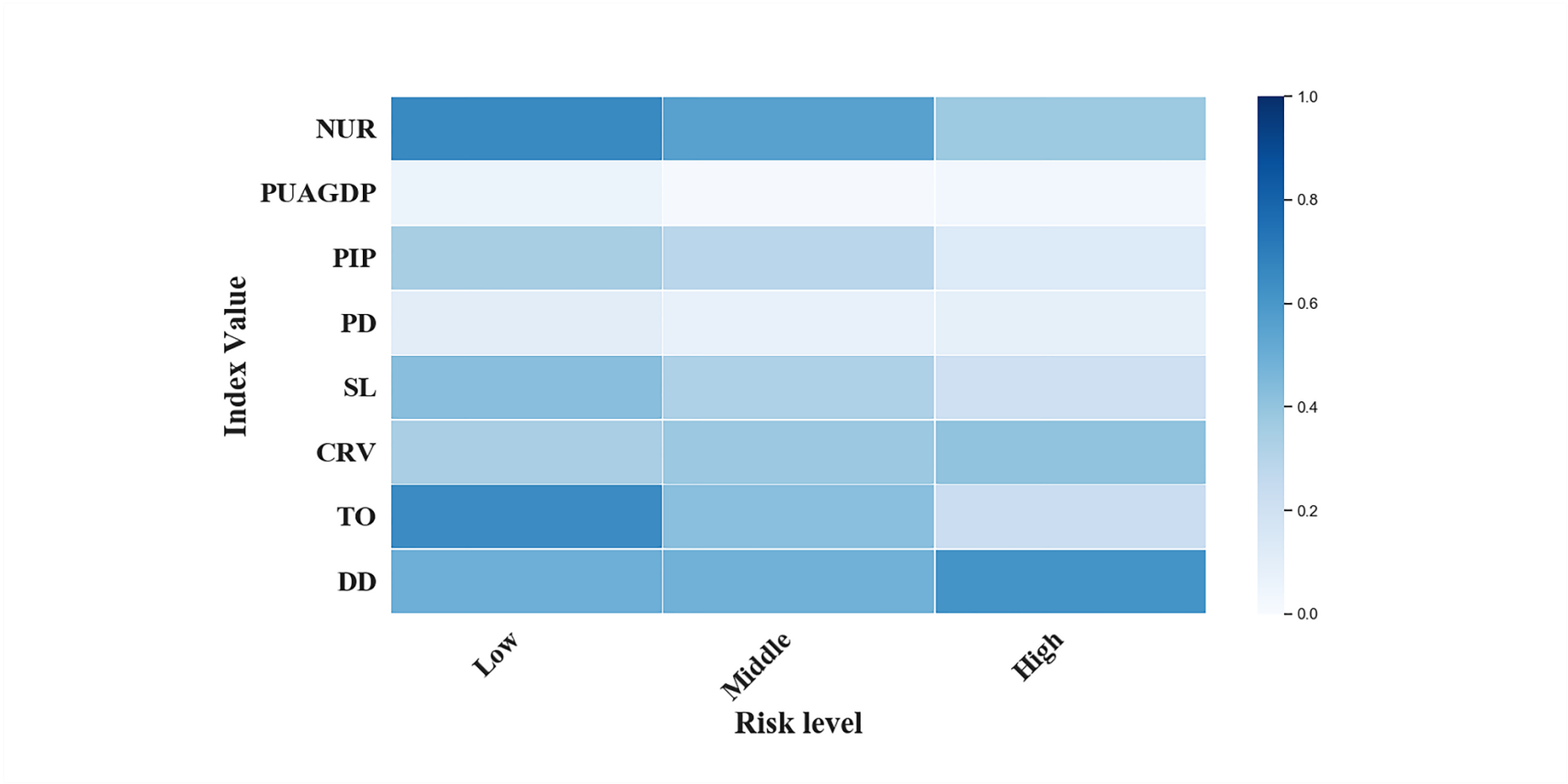
Figure 2



852

853

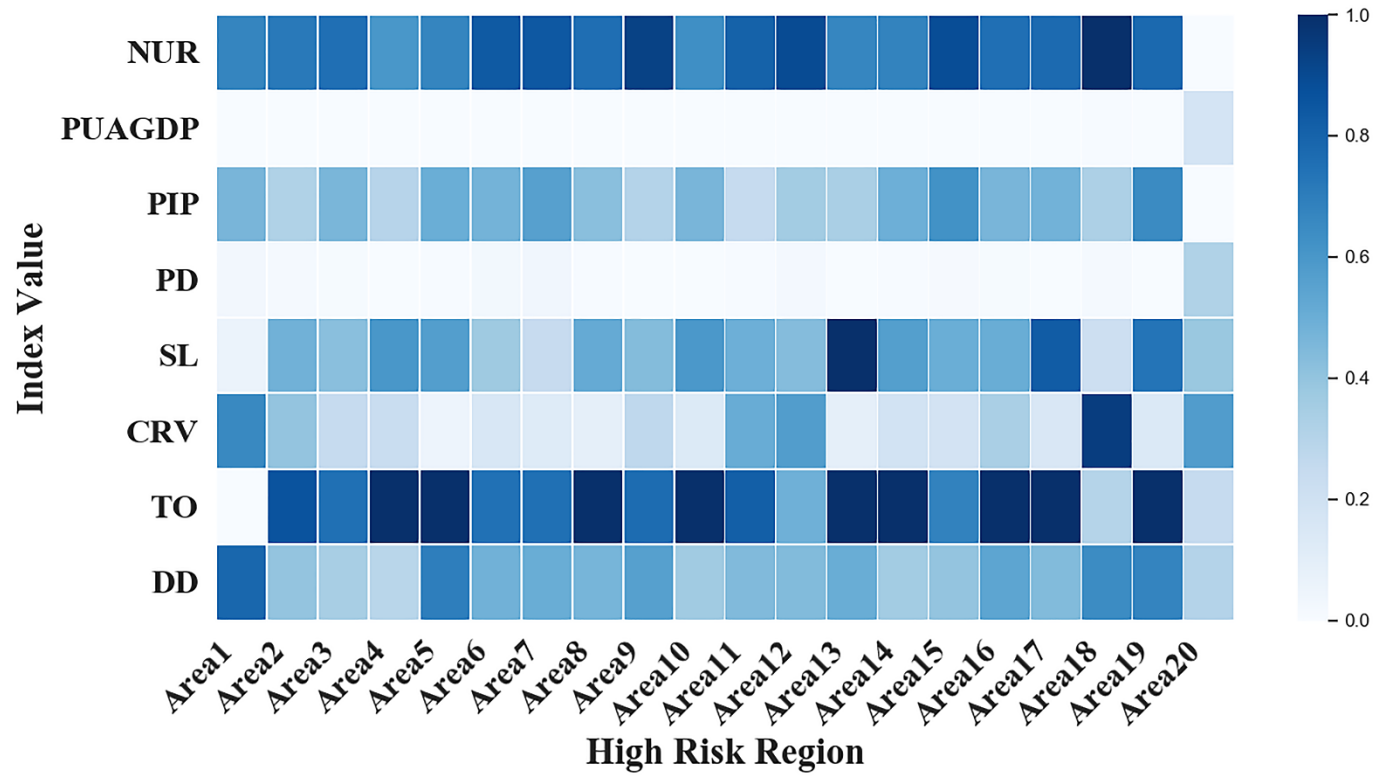
Figure 3



854

855

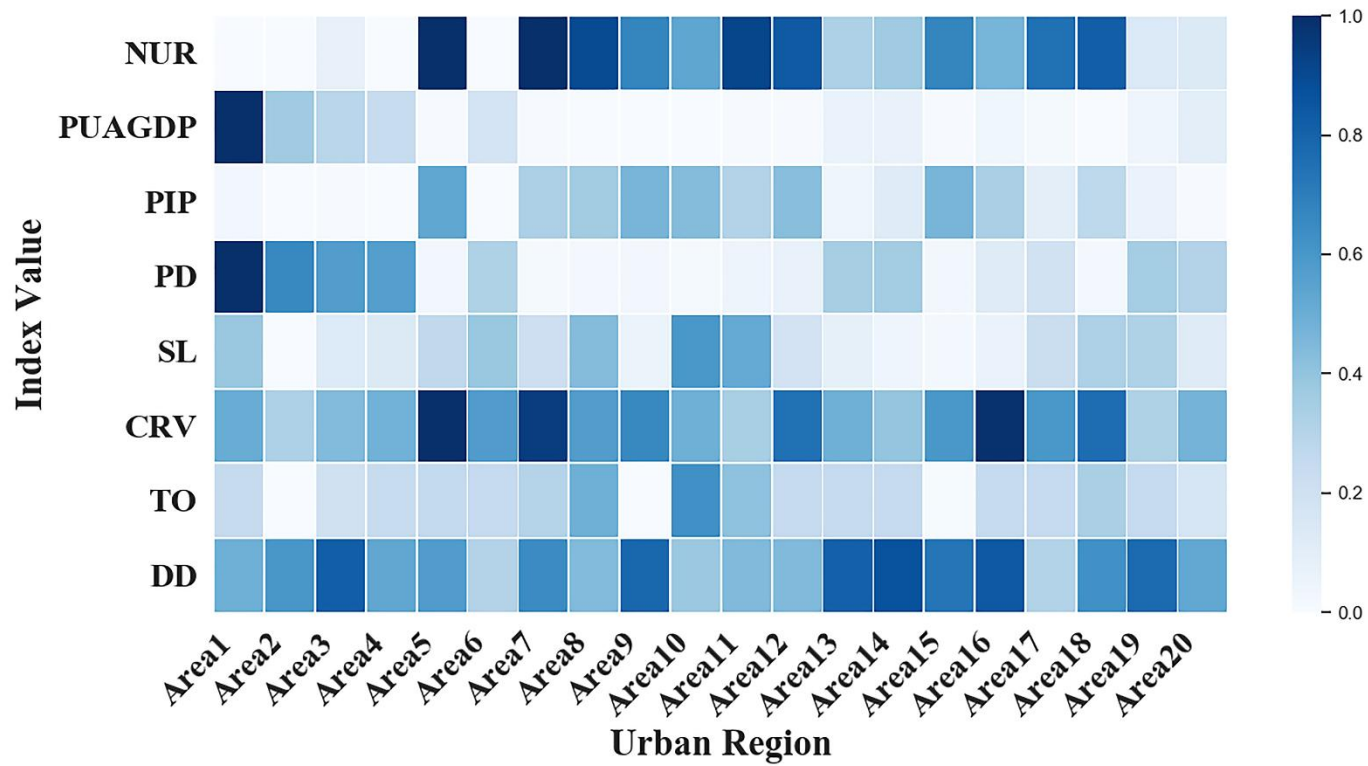
Figure 4



856

857

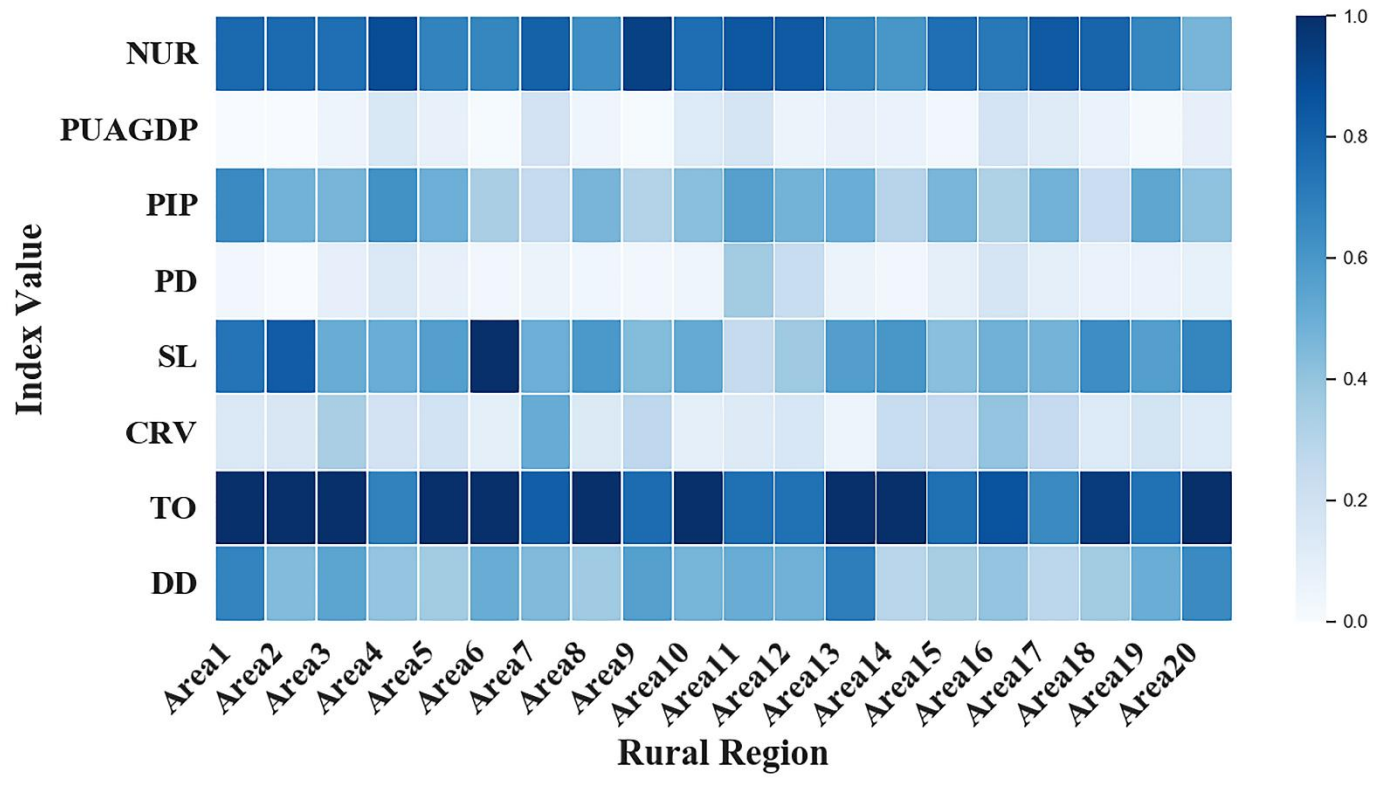
Figure 5



858

859

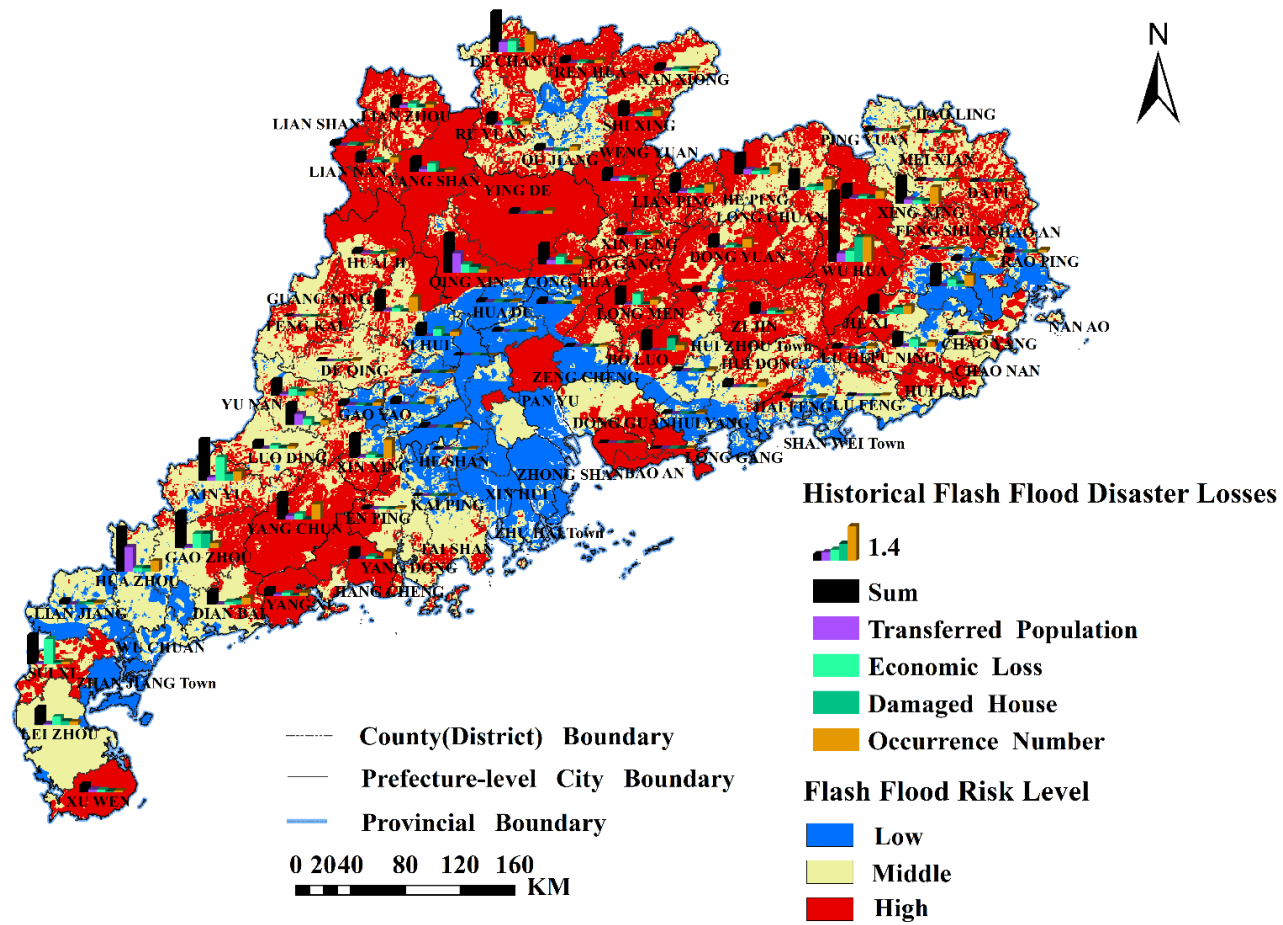
Figure 6



860

861

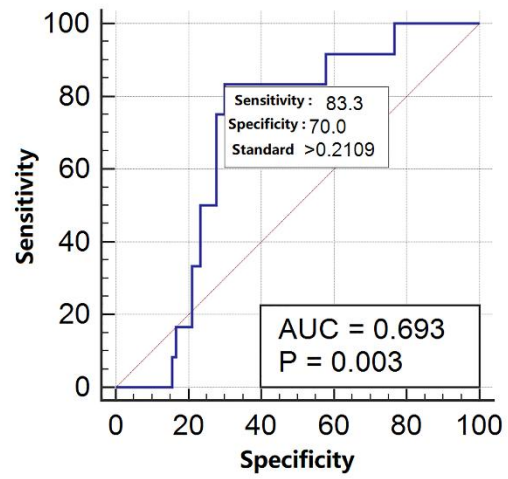
Figure 7



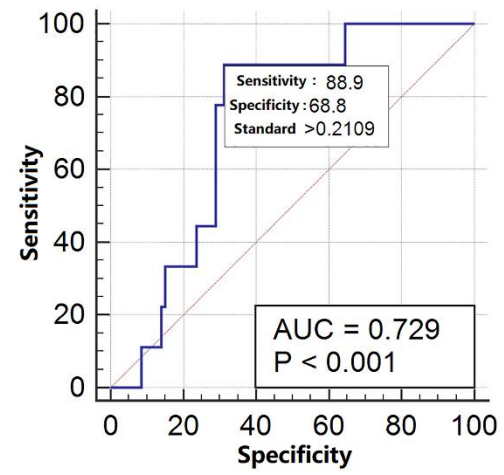
862

863

Figure 8



(a)

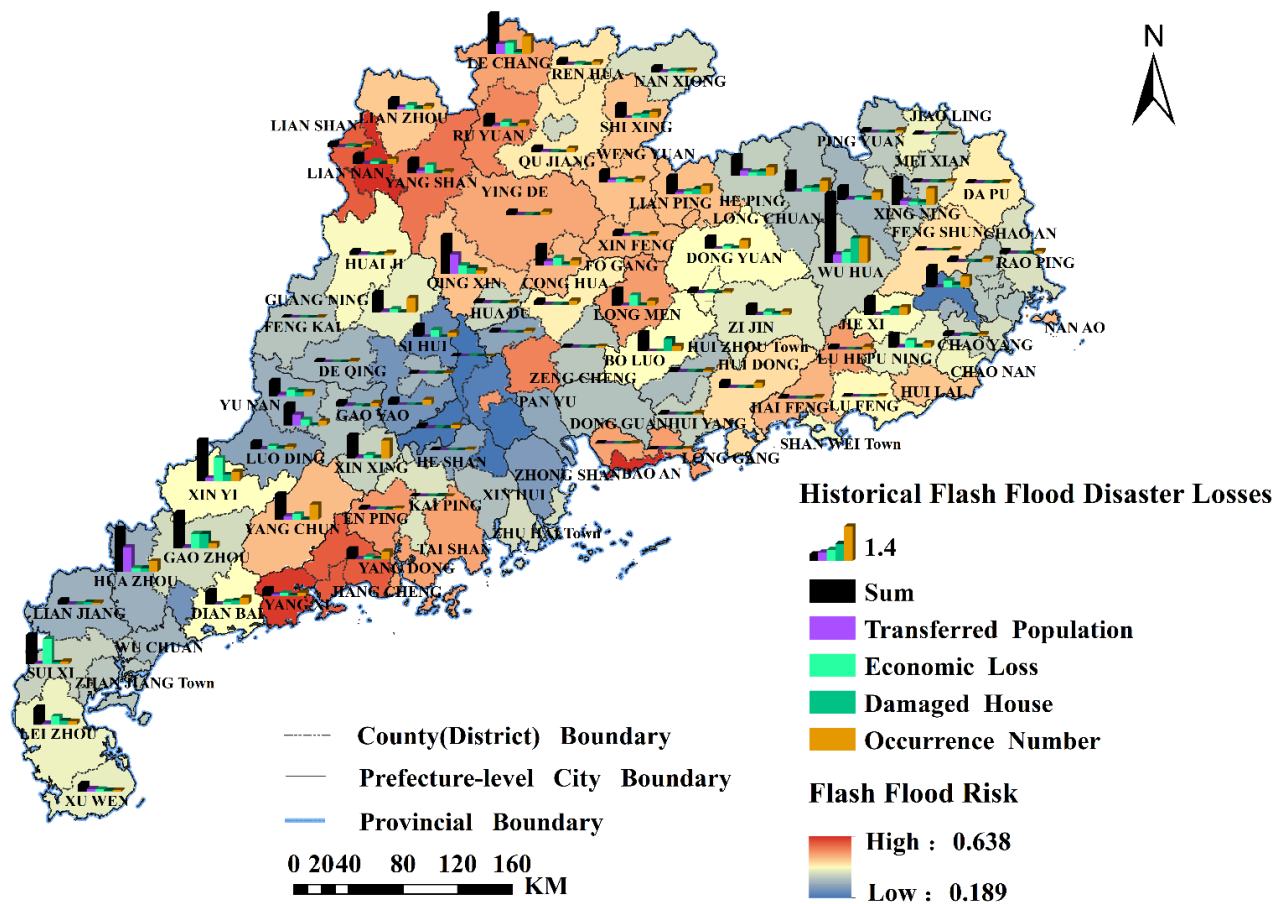


(b)

864

865

Figure 9



866

867

Figure 10

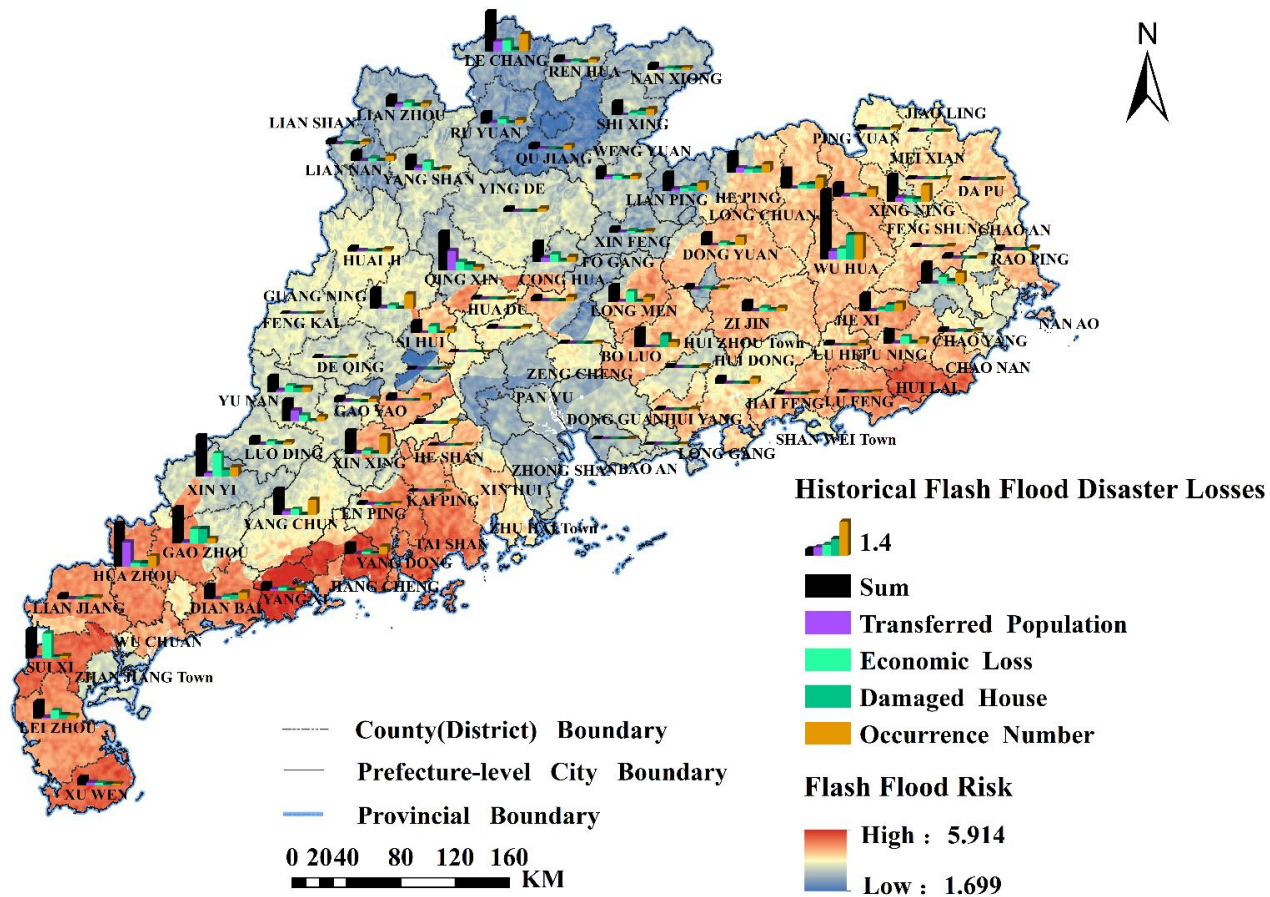


Figure 11

868

869